Morphological evolution of silicon ablated via nanosecond pulsed laser

MING GUO[1,2], YONG-XIANG ZHANG[3,*], NAN LI[1,2], JI-XING CAI[4]

[1]*Jilin Engineering Normal University, Institute for Interdisciplinary Quantum Information Technology, Changchun 130052, China*

[2]*Jilin Engineering Laboratory for Quantum Information Technology, Changchun 130052, China*

[3] *Changchun Institute of Electronic Science and Technology, Changchun 130000, China*

[4]*Changchun University of Science and Technology, Changchun 130022, China*

In order to explore the laws and mechanisms of the microstructure and ablation of silicons irradiated via nanosecond pulsed lasers, a nanosecond laser with a wavelength of 1064 nm was used to irradiate intrinsic silicon and p-type, boron-doped silicon targets. The irradiated morphology of the silicons under different laser conditions was investigated, and the influence of laser energy density, pulse number, incident angle, and target thickness on the cleavage and ablation morphology was analyzed. This study can provide a basis for laser precision machining as well as for understanding the resistance of silicon-based devices to laser damage.

(Received May 21, 2021; accepted February 11, 2022)

Keywords: Silicon, Nanosecond laser, Cleavage, Ablation

1. Introduction

High speed and precise laser applications put an urgent need for new laser technology. Laser applications are mainly realized through the interaction between laser and matter, these applications include laser processing, laser weapons, laser treatment, and laser detection, which are widely used in optical measurements, imaging, satellites, and several other fields. Monocrystalline silicon is the most extensively utilized material for microelectronic devices. It is often used both as a substrate and a filter and plays an important role in high circuit integration and laser system design. The requirements of silicon parameters vary greatly depending on the application field, such as chips, solar cells, and photodetectors. Therefore, it is urgent to carry out research on the effect of the parameters of monocrystalline silicon on lasers. Compared with ultrashort lasers, nanosecond pulsed lasers have higher energy. Furthermore, they exhibit a higher peak power density than long pulse lasers and have an impact pressure on the migration of molten silicon. Nanosecond pulsed lasers can be combined with long and ultrashort pulses to improve the morphology and structure.

Theoretical and experimental research on the effect of nanosecond lasers on silicons has been conducted both nationally and internationally[1-3]. Xueming LV et al used nanosecond lasers and millisecond laser to irradiate intrinsic silicon materials [4], ablation depth and surface damage radius under different laser parameters were studied, compared and analyzed the effect of combined laser and single pulse lasers. Acosta-Zepeda C et al. established a melting simulation model using the enthalpy of fusion and the moving interface equation in heat transfer [5]. Surface morphology of the silicon wafers using a single nanosecond laser was studied, and accurately analyzed the flow after melting. Additionally, they conducted several experiments under different conditions, including different wavelengths. Sardar M et al. studied the irradiation morphology and photoelectric properties of silicon under the action of multi-pulse nanosecond lasers [6]. They used a constant energy density of 7.5 J/cm^2 to analyze the impact of the number of pulses on the surface structure of craters, microcracks, holes, clusters, etc. in an air environment, and found that the performance of silicon remained good after multiple pulses. Zhang J et al. used finite element simulations and experiments to study the ablation of silicon via nanosecond pulsed lasers. Additionally, they prepared high-precision surface microstructures on the silicon surface exhibiting anti-reflection properties in a wide wavelength range from 400 to 2000 nm[7].

In this work, a near-infrared nanosecond pulsed laser was used to irradiate intrinsic silicon and p-type boron-doped silicon to study the influence of the thickness of silicon, laser energy density, and number of pulses on the damaged surface morphology. Furthermore, the damage caused by laser reaming was analyzed, and the conditions that produce cleavage damage were explored. The results provide a basis for the study of long-short pulse laser action on silicon and provide technical reference for laser processing.

2. Experiment

The experimental setup used to investigate the damage caused by a nanosecond pulsed laser to the silicon is shown in Fig. 1. A Vlite-300 dual-pulse solid-state laser from Leibao was used for the experiment. The wavelength of the laser was 1064 nm and width was 12 ns. The laser beam is split by the beam splitter, one beam travelled to the VEGA FL500A energy meter to measure the laser energy, while the other beam was perpendicularly incident onto the surface of the silicon sample through the focusing lens. The radius of the focused laser were 1.0 and 1.5 mm. The silicon sample was clamped on a three-dimensional translation stage.

The experiment was carried out in an air environment, with an ambient temperature of 19 °C, a relative humidity of 30%, and an air pressure of 10^5 Pa. Two types of silicon target material were used in the experiment. The first type consisted of intrinsic silicon, polished on both sides, with a crystal plane orientation of (100). This sample had a size of 20 × 20 mm^2, a resistivity greater than 10 kΩ·cm, and thicknesses is 0.5 and 1.0 mm. The second type consisted is p-type boron-doped silicon, with size of 20 × 20 mm^2, resistivity of 1-30 Ω·cm, and thicknesses is 0.5mm, 1.0mm, and 2.0 mm.

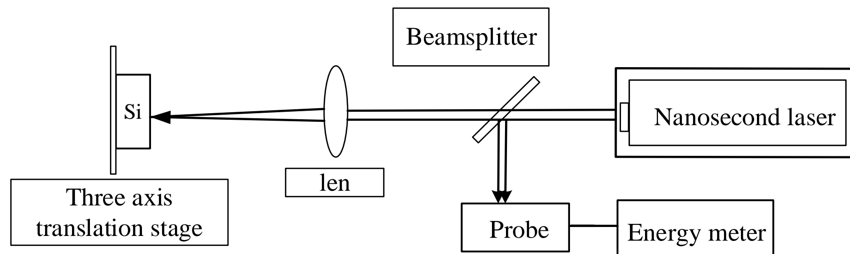

Fig. 1. Experimental setup used for laser ablation of the silicon sample

3. Results and analysis

Fig. 2, Fig. 4, and Fig. 5 were obtained by DMI-5000M Leica metallurgical microscope.

Fig. 2 shows the damage morphology of intrinsic silicon for different laser energy densities. These images were acquired with a spot radius of 1.5 mm and the sample thickness is 1.0 mm. It can be seen from Fig. 2: (1) The cleavage structure is not observed under single pulse laser conditions, and the silicon is mainly thermally damaged by the nanosecond laser; (2) For a low laser energy density, a clear mesh cross-connected structure can be observed.

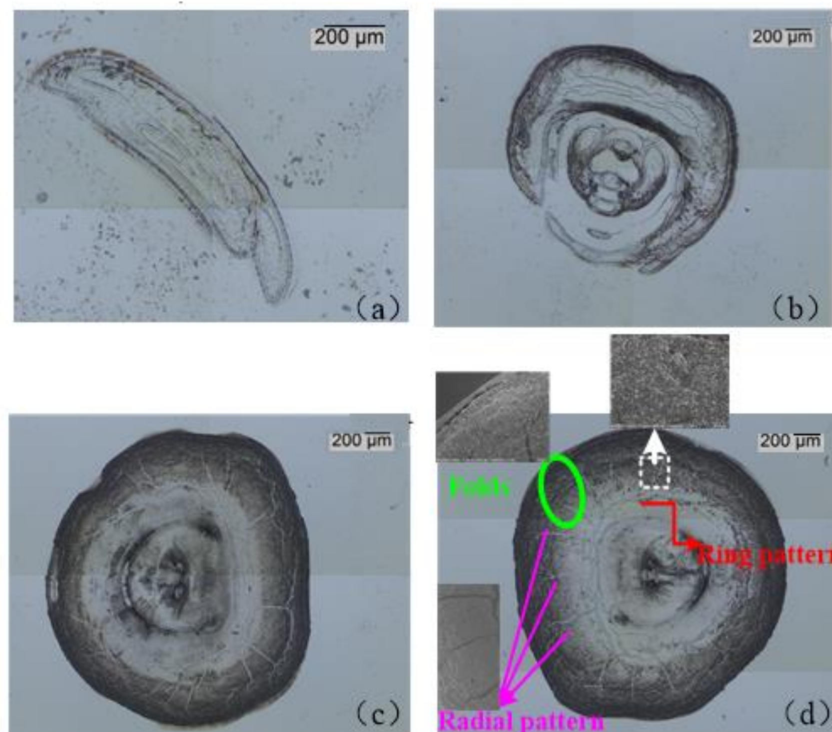

Fig. 2. Damage morphology of intrinsic silicon. (a)1.32J/cm², (b)1.83J/cm², (c)3.21J/cm², (d)3.64J/cm²) (color online)

Upon absorption of the laser energy, the temperature of the silicon target rises, additional thermal stresses occur during its internal expansion, and its edge temperature gradient becomes too large to form microcracks. The target material boils locally to form bubbles, and, after rupture, pits are formed on the surface [8]. As the laser energy density increases, the degree of ablation becomes more severe, and the damage area increases. As the energy density reaches 3.64 J/cm^2, the pit depth increases. After the silicon is eroded, the mechanical strength is suddenly unloaded, and tensile stress originates around the pit. This tensile stress exceeds the fracture strength at the response temperature to produce ring-shaped cracks. Radial and annular cracks appear starting from the center towards the outside, and ripples formed by the melt flow are observed at the edges. Particles appear on the surface of the silicon target. Since the energy density of the irradiating laser is very high, the laser causes the silicon target to generate a plasma. The recoil pressure of the plasma expansion causes all the liquid substances produced during the laser action to sputter out, and a clear surrounding particle splash phenomenon takes place.

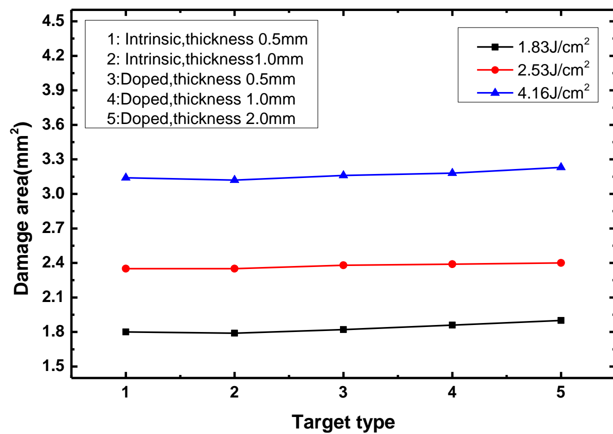

Fig. 3. Damage area of the five silicon materials (color online)

Fig. 3 shows the damage area of the five target materials for different laser energy densities. The first and second target materials are intrinsic silicon with thicknesses of 0.5 and 1.0 mm, respectively, while the third, fourth, and fifth target materials are boron-doped silicon with thicknesses of 0.5, 1.0, and 2.0 mm, respectively. In this case, the laser spot radius was set to 1.0 mm. Overall, when the laser energy density is fixed, the difference in the damage area of the five target materials within 0.1 mm^2. From Fig. 3, the following considerations can be inferred. (1) The boron-doped silicon has a larger damage area than the intrinsic silicon. Compared with the intrinsic silicon, the 0.5mm-thick boron-doped silicon has an average increase in the damage area of 0.02 mm^2, while the 1.0mm-thick boron-doped silicon has an average increase in the damage area of 0.02 mm^2, while the 1.0mm-thick boron-doped silicon has an average increase of 0.05 mm^2. When the laser acts on the silicon target material, the temperature of the irradiated area rises rapidly, and an intrinsic excitation occurs after the energy is absorbed. In the case of the boron-doped silicon, the boron impurity level enters the forbidden band of silicon at a position close to the valence band [9]. The valence band electrons can easily absorb energy and jump to these energy levels, so that the photons below the band gap can also be absorbed. Thus, laser damage is more likely to be caused in doped borosilicate targets than in intrinsic silicon. [2] The damage area of the intrinsic silicon targets of the two thicknesses is basically the same. For doped silicon with different thicknesses, the average damage area of 1.0mm thickness is higher than 0.5mm thickness of 0.02mm^2. After silicon absorbs laser energy, the thermal conductivity is bigger, and the energy is distributed inside the silicon. For thin targets, the target thermal diffusion will occur on the back surface and energy will be lost, so the damage is weaker than thick targets.

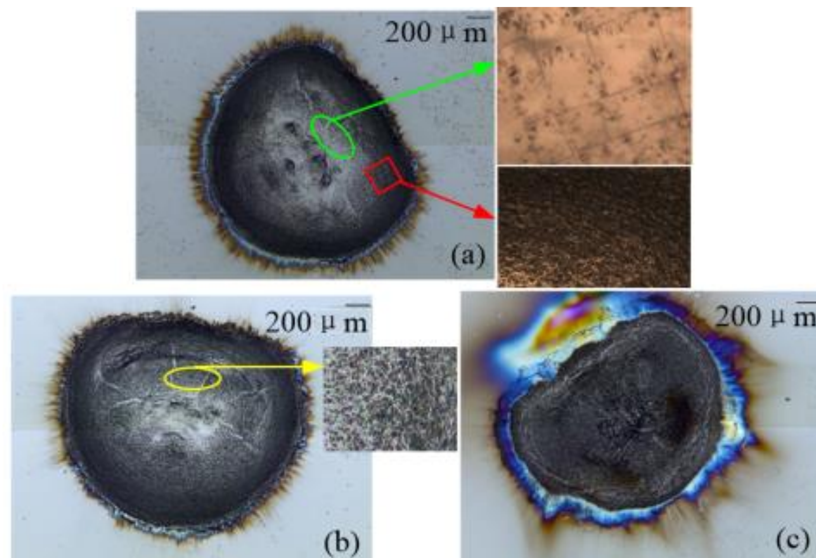

Fig. 4. Damage morphology under pulse train laser conditions. ((a) 4.44J/cm^2 ,(b)5.90J/cm^2, (c)8.92/cm^2) (color online)

Fig. 4 shows the damage morphology of intrinsic silicon for a spot radius of 1.0 mm and a train of five laser pulses. It can be seen from Fig. 4, when the laser energy density reaches 4.44 J/cm^2, a clear cleavage morphology is observed, with cleavage cracks assuming a “cross” shape. Monocrystalline silicon is anisotropic and has a typical diamond structure [10], the distance between the (111) crystal planes is large, the bonding force between the planes is weak, and the cleavage fracture is the most likely to occur. In the experiment, a monocrystalline silicon sample with a (100) crystal plane orientation was used, the angle between the (111) crystal plane and the (100) crystal plane is 90°. When a cleavage fracture occurs, a "cross" crack is formed on the (100) crystal planes. As the laser energy density increases, the cleavage area is covered by the thermally damaged area, and ablation is intensified. When the laser energy density reaches 8.92 J/cm^2, severe ablation and splashing occur, the damage area becomes larger, and the edge of the irradiated area is fragmented. During an intense ablation process, the electrons of the silicon atoms undergo transitions and release energy in the form of photons. The frequencies of the photons released by electrons at different levels are different, forming a color spectrum on the silicon surface.

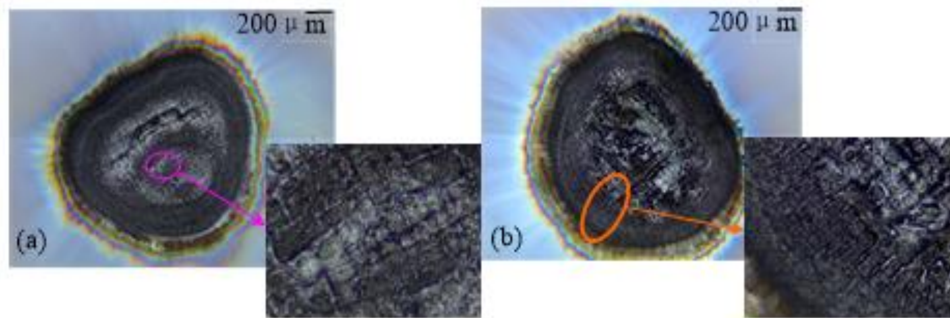

Fig. 5. Cleavage damage morphology under pulse train. laser. ((a)3.16J/cm^2, (b)4.44J/cm^2)

When the number of laser pulses is increased to 20 with an energy density of 3.16 J/cm^2, a clear ablation takes place and a coexisting cleavage structure appears. As shown in Fig. 5, the cleavage appears in the form of vertical cleavage lines. This is due to the fact that monocrystalline silicon has a double-layer close-packed surface structure, with the {111} planes being double-layer close-packed surfaces. The atomic binding force in the close-packed surface is strong, the distance between the surfaces is large, and the binding force is weak, thus, the crystal can be easily split along the {111} crystal planes, and 90° cleavage lines are formed on the crystal surface. This is different from the damage pattern obtained for intrinsic silicon via millisecond pulse laser. The cleavage structure caused by long pulse laser only appears on the edges of the ablation region, where no severe ablation has occurred. Since the duration of a single nanosecond pulse laser is 12 ns, the laser energy is not sufficiently high even for 20 pulses, and the degree of ablation is not large enough to cover the cleavage structure.

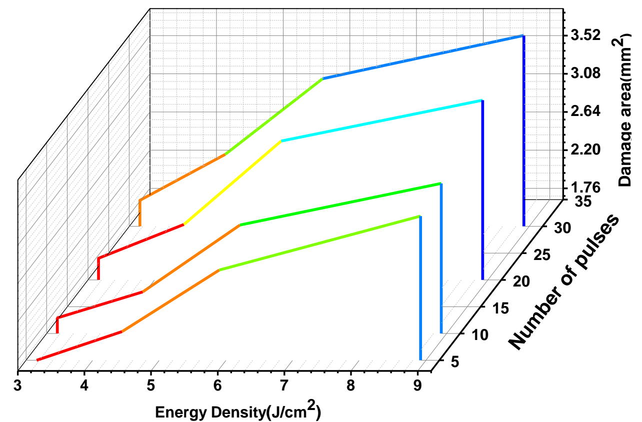

Fig. 6. Damage area of intrinsic silicon under pulse train laser (color online)

Fig. 6 shows the damage area of intrinsic silicon under pulsed train laser conditions with a spot radius of 1.0 mm. For a fixed number of pulses, as the laser energy density increases, the intrinsic silicon damage area increases. Furthermore, as the number of pulses increases, the damage area increases rapidly due to the cumulative effect of temperature and stress. When the number of pulses increases from 5 to 30, the damage area is averaged under the four laser energy density conditions illustrated in the figure. In this case, an increase of 21.3% is observed.

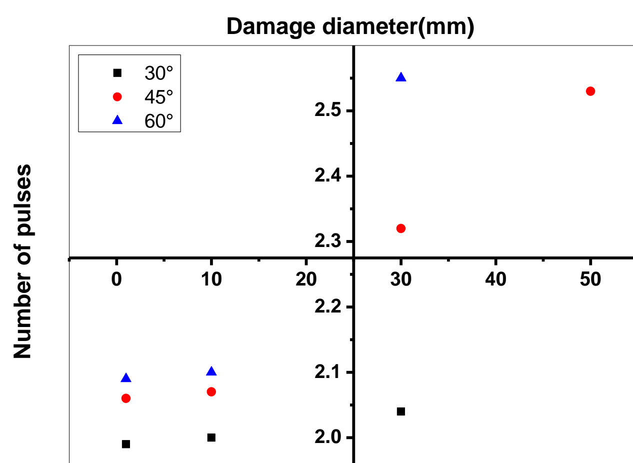

Fig. 7. Damage diameter for different laser incident angles and numbers of pulses (color online)

In laser technology, such as laser perforation, nanosecond lasers can be used alone as a laser source for irradiation or can be used in combination with long pulse or continuous lasers for reaming. Therefore, lasers are required to act on the target from different directions. Fig. 7 shows the damage diameter of intrinsic silicon under laser irradiation at different incident angles. In this case, the spot radius was 1.0 mm, and the laser energy density was 9.4 J/cm^2. When the incident angle changes from 30° to 60°, the damage diameter changes from 1.99 to 2.09 mm for single pulse laser. When the number of pulses increases to 30, the damage diameter changes from 2.04 to 2.55 mm. As the number of pulses increases, the damage diameter increases approximately linearly. When the beam is incident at a certain oblique angle, the optical path of the beam reaching the target surface becomes longer, and the light intensity distribution of the spot changes. The damage to the edge of the beam first reaching the target surface is aggravated, and the damage range extends outwards along the target edge. As the number of pulses increases, a clear energy accumulation occurs [12] due to the heat accumulation effect, and the damage area increases rapidly.

4 Conclusions

Using a near-infrared nanosecond pulsed laser to irradiate intrinsic silicon and p-type silicon, the ablation morphology of silicons and the mechanism of the induced damage were studied. Additionally, the influence of the silicon target thickness, laser energy density, pulse number, and other parameters on the induced damage was investigated. Under single pulse laser conditions, the laser energy density was increased from low to high, and no cleavage damage structure appeared. 90° cleavage lines were observed under specific energy density pulse train conditions. The silicon target material absorbs the laser energy, which is transformed into thermal energy, causing boiling of the system, bubbles are then produced and burst to form erosion pits. The stress generated by the temperature gradient causes cracks on the surface. Two types of cracks were observed namely radial and annular cracks, initiating from the center of the target towards the edges. Silicon targets doped with boron were found to be more susceptible to damage than intrinsic silicon. As the number of pulses increased, the damage area increased rapidly due to the cumulative effect of temperature and stress. When the laser incident angle was changed from 30° to 60°, the damage diameter increased. These results lay the foundation for the processing of silicon-based optoelectronic devices.

Acknowledgments

The research is supported by "Science and Technology Development Plan Project of Jilin Province (Grant No. YDZJ202101ZYTS178)", "Youth Science Fund Project in the National Natural Science Foundation of China (Grant No. 61905089)", "Youth Science Fund Project in the National Natural Science Foundation of China (Grant No.62005023)", "Specialized Fund for the Doctoral Research of Jilin Engineering Normal Universi ty(Grant No.BSKJ201824).

References

[1] S. V. Starinskiy, A. A. Rodionov, Y. G. Shukhov, Applied Surface Science **512**, 145753 (2020).
[2] M. Sardar, C. Jun, Z. Ullah et al., Applied Optics **57**(6), 1296 (2018).
[3] M. E. Shaheen, J. E. Gagnon, B. J. Fryer, Optics and Lasers in Engineering **119**, 18 (2019).
[4] X. Lv, Y. Pan, Z. Jia, Z. Li, X. Ni, Applied Optics **56**(17), 5060 (2017).
[5] C. Acosta-Zepeda, P. Saavedra, J. Bonse, E. Haro-Poniatowski, Journal of Applied Physics **125**(17), 175101 (2019).
[6] M. Sardar, J. Chen, Z. Ullah, M. Jelani, A. Tabassum, J. Cheng, Y. Sun, J. Lu, Materials Research Express **4**(12), 125902 (2017).
[7] J. Zhang, L. Zhao, A. Rosenkranz, C. Song, Y. Yan, T. Sun, Journal of Micromechanics and Microengineering **29**(7), 075009 (2019).
[8] Qisheng Lu, Tian Jiang, Houman Jiang, Laser radiation effects on semiconductor materials and devices, National Defense Industry Press, 2015.
[9] Cheng-Wei, Qi-Sheng Lu, Zheng-Xiu Fan, Laser irradiation effect, National Defense Industry Press, 2002.
[10] Zhichao Jia, Tingzhong Zhang, Huazhong Zhu, Zewen Li, Zhonghua Shen, Jian Lu, Chinese Optics Letters **16**(1), 011404 (2018).
[11] Zhichao Jia, Zewen Li, Xueming Lv,, Xiaowu Ni, Applied Optics **56**(17), 4900 (2017).
[12] Peng Sun, Mo Li, Qing-Xin Yang, Journal of Terahertz Science and Electronic Information Technology **16**(1), 158(2018).

* Corresponding author: laserqit@sina.com